Received: 5 September 2018 | Revised: 27 December 2018 | Accepted: 26 February 2019

DOI: 10.1002/hipo.23088

WILEY

RESEARCH ARTICLE

Electroacupuncture in rats normalizes the diabetes-induced alterations in the septo-hippocampal cholinergic system

Virginia Protto[1] | Marzia Soligo[1] | Maria Egle De Stefano[2] | Stefano Farioli-Vecchioli[3] | Lionel N. J. L. Marlier[1] | Robert Nisticò[4,5] | Luigi Manni[1]

[1]Institute of Translational Pharmacology, Consiglio Nazionale delle Ricerche (CNR), Rome, Italy

[2]Department of Biology and Biotechnology "Charles Darwin", Sapienza University, Rome, Italy

[3]Institute of Cell Biology and Neurobiology, Consiglio Nazionale delle Ricerche (CNR), Rome, Italy

[4]Pharmacology of Synaptic Disease Lab, European Brain Research Institute (EBRI), Rome, Italy

[5]Department of Biology, University of Rome Tor Vergata, Rome, Italy

Correspondence
Luigi Manni, Institute of Translational Pharmacology, Consiglio Nazionale delle Ricerche (CNR), via del Fosso del Cavaliere 100, 00133 Rome, Italy.
Email: luigi.manni@ift.cnr.it

Abstract

Diabetes induces early sufferance in the cholinergic septo-hippocampal system, characterized by deficits in learning and memory, reduced hippocampal plasticity and abnormal pro-nerve growth factor (proNGF) release from hippocampal cells, all linked to dysfunctions in the muscarinic cholinergic modulation of hippocampal physiology. These alterations are associated with dysregulation of several cholinergic markers, such as the NGF receptor system and the acetylcholine biosynthetic enzyme choline-acetyl transferase (ChAT), in the medial septum and its target, the hippocampus. Controlled and repeated sensory stimulation by electroacupuncture has been proven effective in counteracting the consequences of diabetes on cholinergic system physiology in the brain. Here, we used a well-established Type 1 diabetes model, obtained by injecting young adult male rats with streptozotocin, to induce sufferance in the septo-hippocampal system. We then evaluated the effects of a 3-week treatment with low-frequency electroacupuncture on: (a) the expression and protein distribution of proNGF in the hippocampus, (b) the tissue distribution and content of NGF receptors in the medial septum, (c) the neuronal cholinergic and glial phenotype in the septo-hippocampal circuitry. Twice-a-week treatment with low-frequency electroacupuncture normalized, in both hippocampus and medial septum, the ratio between the neurotrophic NGF and its neurotoxic counterpart, the precursor proNGF. Electroacupuncture regulated the balance between the two major proNGF variants (proNGF-A and proNGF-B) at both gene expression and protein synthesis levels. In addition, electroacupuncture recovered to basal level the pro-neurotrophic NGF receptor tropomyosin receptor kinase-A content, down-regulated in medial septum cholinergic neurons by diabetes. Electroacupuncture also regulated ChAT content in medial septum neurons and its anterograde transport toward the hippocampus. Our data indicate that repeated sensory stimulation can positively affect brain circuits involved in learning and memory, reverting early impairment induced by diabetes development. Electroacupuncture could exert its effects on the septo-hippocampal cholinergic neurotransmission in diabetic rats, not only by rescuing the hippocampal muscarinic responsivity, as previously described, but also normalizing acetylcholine biosynthesis and NGF metabolism in the hippocampus.

KEYWORDS

basal forebrain cholinergic system, diabetic encephalopathy, electroacupuncture, nerve growth factor, rats

1 | INTRODUCTION

The septo-hippocampal cholinergic neurotransmission has an important role in cognitive processes (Baxter, Bucci, Gorman, Wiley, & Gallagher, 2013; Sarter, 2015). Inputs from basal forebrain cholinergic nuclei (BFCN) regulate the intrinsic hippocampal network function (Teles-Grilo Ruivo & Mellor, 2013), and control important features of hippocampal cellular physiology (Cooper-Kuhn, Winkler, & Kuhn, 2004; Mohapel, Leanza, Kokaia, & Lindvall, 2005; Van der Borght et al., 2005). Deficits in the cholinergic transmission can potentially influence all aspects of cognition and

behavior, related to cortical and hippocampal information processing (Ferreira-Vieira, Guimaraes, Silva, & Ribeiro, 2016). Indeed, alterations in the central cholinergic system functionality have been pointed as an important factor in many forms of cognitive impairments, including those developing in diabetic encephalopathy (DE) (Biessels, Kappelle, Bravenboer, Erkelens, & Gispen, 1994; Welsh & Wecker, 1991).

The neurotrophin nerve growth factor (NGF) is an important regulator of the septo-hippocampal physiology and has been pointed as a possible therapeutic in neurodegenerative diseases characterized by a prominent cholinergic deficit (Aloe, Rocco, Bianchi, & Manni, 2012). NGF is produced by the hippocampus as a pro-peptide (proNGF), which can influence the physiology of both hippocampal cells themselves (Guo et al., 2013) and cholinergic neurons of the medial septum (MS) projecting to hippocampus (Whittemore et al., 1988). ProNGF can be processed by intracellular and/or extracellular proteases in a mature peptide (mNGF), which acts as a potent neurotrophic factor on the same cell systems (Hempstead, 2014). Mature and proNGF activate, with different affinities, a receptor system composed by the tropomyosin receptor A (TrkA) and the p75 neurotrophin receptor ($p75^{NTR}$) (Wehrman et al., 2007), whose triggering mainly results in neurotrophic outcomes (Masoudi et al., 2009). Only proNGF challenges the $p75^{NTR}$-sortilin receptor complex, activating a proapoptotic intracellular signaling cascade (Nykjaer et al., 2004).

We recently demonstrated that the physical therapy electroacupuncture (EA) was effective in counteracting major hippocampal neurophysiological dysfunctions induced in young adult rats by diabetes (Rocco et al., 2013; Soligo et al., 2017). In particular, the repeated sensory stimulation elicited by EA corrected diabetes-induced alterations in spatial learning and memory, the decrease in hippocampal dentate gyrus long-term-potentiation (DG-LTP) and the increase in proNGF release by hippocampal cells, probably by regulating the activity of the M1 muscarinic acetylcholine (Ach) receptor (M1AchR) subtype (Soligo et al., 2017).

In the present work, we aimed at further characterizing the effects of diabetes and EA on the septo-hippocampal system neurophysiology in diabetic rodents. Dysfunctions in the interplay between Ach neurotransmission and NGF synthesis and release could be of central importance in the establishment of cholinergic sufferance (Cuello, Bruno, Allard, Leon, & Iulita, 2010). As we had indications that EA could specifically act on this Ach-NGF dynamics (Rocco et al., 2013; Soligo et al., 2017), we first explored the effects of experimental diabetes and EA on the balance between different proNGF variants and between proNGF and mNGF in the hippocampus. We then analyzed the differences in phenotypic composition of both HP and MS, mainly focusing on the neuronal cholinergic phenotype, known to be regulated by NGF (Hefti, 1986).

2 | METHODS

2.1 | Animals

Animal care procedures were conducted in conformity with the Italian Legislation and the European Union Directive (Italian Legislative Decree 26/2014 and 2010/63/EU). Animals were subjected to experimental protocols approved by the Veterinary Department of the Italian Ministry of Health (Permit Number: 192/2015–PR). All experiments were conducted according to the ARRIVE guidelines (Kilkenny, Browne, Cuthill, Emerson, & Altman, 2010). All adequate measures were taken to minimize animal pain or discomfort and all surgery was performed under isoflurane anesthesia. Young adult male Sprague–Dawley rats weighting 150–174 g were purchased from Envigo (Bresso, Italy). Animals were housed three per cage in a controlled room (temperature: 21 ± 1°C; average lux: ≈ 100 lx; humidity: 50 ± 5%) with a 12 hr light/12 hr dark cycle. Rats had *ad libitum* access to food and water for all the experiments.

2.2 | Study design and diabetes induction

Randomization was carried out using the online Research Randomizer Program (www.randomizer.org), so that the persons carrying out tissue processing, data acquisition, and statistical analysis were blind to the treatment. The GPower program (http://www.gpower.hhu.de/en.html) was used to calculate samples size, according to the statistical methodologies used to compare means (see Section 2.10 below). Differences among the compared means ≥30% with $SD \leq 20\%$ of the mean within groups have been considered to obtain a power of at least 80% with an alpha level of 0.05. Two months old rats were randomly divided in three groups as follow: control rats (vehicle-treated, ctr group), diabetic rats (streptozotocin-treated, STZ group), diabetic rats treated with electroacupuncture (STZ- and electroacupuncture-treated, STZ + EA group). Hyperglycemia was induced by a single intraperitoneal injection of 65 mg/kg STZ dissolved in 20 mmol/L citrate buffer (100 mM – 36 mM citric acid and 64 mM di-sodium hydrogen phosphate) pH 4.5 (vehicle). One week after streptozotocin treatment, the establishment of hyperglycemia was checked by an Accutrend™ GC (Roche Diagnostic, Mannheim, Germany) glucose analyzer. Rats with blood glucose levels above 300 mg/dL were allocated to the diabetic experimental groups. The EA treatment was performed on diabetic animals twice a week for 3 weeks, starting 1 week after diabetes induction. The rats were euthanized after 4 weeks of diabetes (1 day after the last EA treatment). Six to eight rats for each experimental group were euthanized by decapitation, under light isoflurane anesthesia. The brains were rapidly dissected on ice and the dissected areas snap-frozen in liquid nitrogen and stored at −80°C. Three to five rats for each experimental group were terminally anesthetized according to institutional animal care and use-committee-approved protocol and were intracardially perfused with 4% (wt/vol) paraformaldehyde in PBS and brains were postfixed overnight (ON), cryoprotected in 30% (wt/vol) sucrose dissolved in PBS and followed processing for confocal microscopy.

2.3 | Electroacupuncture treatment

From a Western perspective, EA is a nonpharmacological method known to trigger a number of reactions at spinal level and in the brain (Andersson & Lundeberg, 1995; Sato, Sato, & Uchida, 2002). Low-frequency electroacupuncture (1–4 Hz), with intensity high enough to cause muscle twitches, probably excites low and high threshold mechanoreceptors (Noguchi et al., 1999) and particularly a group of receptors

found in muscles that are physiologically activated during muscle contractions (Kaufman, Longhurst, Rybicki, Wallach, & Mitchell, 1983; Kniffeki, Mense, & Schmidt, 1981). It has been suggested that EA, with repetitive muscle contractions, results in the activation of physiological processes similar to those resulting from physical exercise (Andersson & Lundeberg, 1995). EA stimulation was achieved by inserting stainless steel needles (diameter 0.20 mm), to depths of 0.5–0.8 cm, bilaterally, at the traditional Chinese acupoints Stomach 36 (ST36; at the proximal insertion of the tibialis anterior muscle) and Large Intestine 4 (LI4; in the middle of the right dorsal thenar muscle). Both the acupoints are known to be effective in the activation of central and peripheral NGF system (Aloe & Manni, 2009; Manni, Florenzano, & Aloe, 2011; Pagani, Manni, & Aloe, 2006; Rocco et al., 2013; Stener-Victorin et al., 2000). Low-frequency EA was given to conscious rats, placed in a soft fabric harness and suspended above the desk (Johansson et al., 2010) through a specific electrical stimulator (CEFAR ACUS II; Cefar-Compex Scandinavia, Malmo, Sweden). The acupoints were electrically stimulated at 2 Hz frequency with 0.1-s, 80-Hz burst pulses with 0.8–1.0 mA of intensity. The location and type of stimulation were the same in all animals. Control (ctr) and diabetic (STZ) rats were exposed to the same handling and suspension procedure but not to EA.

Based on our previous studies and supported by the current knowledge about the use of proper controls in acupuncture studies, we decided not to enroll, in our experimental setup, the control + EA group as well as any kind of minimal or EA-treated diabetic rats (Lund & Lundeberg, 2006; Lundeberg, Lund, Sing, & Naslund, 2011; Manni, Aloe, & Fiore, 2009; Rocco et al., 2013). Controls are key factor in acupuncture studies (Lund & Lundeberg, 2006; Lundeberg et al., 2011). It is actually recognized that there is no ideal control treatment in acupuncture studies (Lundeberg et al., 2011). The evidence that needling activates all of the possible afferent fibers type, vanish the use of every control treatment based on minimal, superficial, or sham stimulation. However, it has been suggested that most of the effects of acupuncture are stress-induced (Lundeberg et al., 2011). Thus, where applicable to experimental design, rodents subjected to manipulation procedure, but not to acupuncture, are used as treatment controls. Moreover, as for its effects on healthy subjects, the acupuncture results in increased activity in the limbic structures whereas in patients with pain a deactivation of the same structures is reported (Lundeberg et al., 2011). This would suggest that studies using healthy subjects is of great interest but have limited relevance when a disease-specific therapeutic action of EA is investigated. Furthermore, in previous animal studies investigating the correlation between EA and the brain NGF system (Manni et al., 2009; Rocco et al., 2013), we reported a substantial lack of effects in EA-treated healthy animals, whereas an effect of the physical therapy on brain NGF and on markers of neurodegeneration was noticed (Manni et al., 2009; Rocco et al., 2013).

2.4 | Immunofluorescence

Coronal brain sections (40 μm-thick) were obtained using a cryostat. Free-floating sections were blocked and permeabilized with 10% (vol/vol) donkey serum, 1% (wt/vol) BSA, and 0.3% (vol/vol) Triton X-100 (blocking buffer), for 2 hr at room temperature (RT). Sections were then incubated with primary antibody (detailed in Table 1) diluted in blocking buffer ON at 4°C. Sections were rinsed in PBS and specific secondary antibodies were incubated 2 hr at RT. After extensive washes with PBS, sections were incubated for 10 min with Hoechst reagent for nuclei staining and mounted and coverslipped with Fluoromount (cat F4680, Sigma-Aldrich, St. Louis, MO).

2.5 | Confocal microscopy

Coronal brain sections obtained from three- to five-rats for each group were processed for confocal microscopy. In preparation for an unbiased estimate of cell numbers, an initial tissue section was selected randomly at one anatomic border of the brain region to be estimated. For hippocampus, we analyzed the region that spanned from −2.40/−3.72 mm relative to Bregma according to Paxinos' Rat Brain atlas (Paxinos, 1982), corresponding to the septal hippocampus. To cover this region of interest, stained slices for each rat were analyzed spacing 320 μm from each other. For MS, all the anatomic region that spanned from −0.5/+1.2 mm relative to Bregma was analyzed, processing 1 section every 120 μm. At least three sections were analyzed for each animal in every analysis performed. Stained sections were imaged with a confocal laser-scanning microscope (Leica SP5, Leica Microsystems, Wetzlar, Germany) under sequential mode, to avoid crosstalk between channels. Confocal image acquisition was conducted so that all samples were imaged using consistent settings for laser power and detector gain. Boundaries and subdivisions of the brain structures were identified with reference to the Paxinos' Rat Brain Atlas (Paxinos, 1982). Image analysis was performed by the Imaris Suite 7.4 software (Bitplane A.G., Zurich, Switzerland). An operator blind to the experiment evaluated the distribution of NeuN, GFAP, choline-acetyl transferase (ChAT), TrkA receptor, and $p75^{NTR}$ receptor in the different areas. The number of immunopositive cells was automatically evaluated, using the Imaris Spot module. Cell number obtained for each section was divided for the corresponding area of the section, to obtain the average number of cells per square millimeter.

The Imaris Surface module was used to automatically draw a mask on ChAT immunostaining (Supporting Information Figure S1). The obtained masks were used to evaluate the area covered by the ChAT fibers and to measure the mean pixel intensity of the ChAT immunofluorescence in fibers and cells. The same masks were duplicated for each channel to evaluate the mean pixel intensity of TrkA receptor and $p75^{NTR}$ receptor in $ChAT^{+}$ cells. The same procedure was used to evaluate the pixel intensity of the proNGF that is localized in the neuronal and glial cells ($NeuN^{+}$ and $GFAP^{+}$ immunostaining, respectively). In this analysis, data were expressed as the percentage of the masked proNGF pixel intensity divided on the total proNGF pixel intensity measured in the region of interest.

For production of figures, processing was done by using the Adobe Photoshop CS6 software (Adobe Systems Incorporated, San Josè, CA): production, brightness, and contrast of images were globally enhanced by using linear histogram correction and images were slightly oversaturated.

TABLE 1 Antibodies used

Primary Antibody	Catalogue, Manufacturer	RRID/PMID	Application/Dilution
*rabbit **anti-proNGF** EP1318y*	68151, Abcam	AB_11156445	ELISA detection antibody 1:5000
*mouse **anti-NGF** 27/21*	MAB5260, Millipore	AB_95188	ELISA detection antibody 1:1000
*goat **anti-NGF***	AF-556-NA, R&D	AB_2298544	ELISA capture antibody 0,4 μg/ml
*rabbit **anti-NGF** H20*	548, Santa Cruz biotechnologies	AB_632011	IP 2 μg
*rabbit **anti-NGF** M20*	549, Santa Cruz biotechnologies	AB_632012	WB 1:1000
*rabbit **anti-proNGF***	AB 9040, Chemicon	AB_262175	IF 1:400
*rabbit **anti p75^{NTR}** H92*	5634, Santa Cruz biotechnologies	AB_648183	IF 1:200
*rabbit **anti-TrkA***	sc-118, Santa Cruz biotechnologies	AB_632556	IF 1:50
*mouse **anti-ChAT***	Clone 17, courtesy of Dr. Costantino Cozzari	PMID: 8786796	IF 1:200
*mouse **anti-NeuN***	MAB377, Millipore	AB_2314891	IF 1:400
*mouse **anti GFAP***	556327, BD Pharmigen	AB_396365	IF 1:200

Secondary Antibody	Catalogue, Manufacturer	RRID	Application/Dilution
Anti-rabbit IgG, HRP-linked	P8651, Cell Signaling Technology	AB_2099233	WB 1:4000
Donkey anti Mouse IgG-Alexa Fluor 488 conjugated	R37114, Thermo Fisher Scientific	AB_2556542	IF 1:300
Donkey anti Rabbit IgG-Alexa Fluor 555 conjugated	A-31572, Thermo Fisher Scientific	AB_162543	IF 1:300
Goat anti Mouse IgG-Alexa Fluor 594 conjugated	R-37121, Thermo Fisher Scientific	AB_2556549	IF 1:300
Goat anti Rabbit IgG-Alexa Fluor 488 conjugated	A-11034, Thermo Fisher Scientific	AB_2576217	IF 1:300

ELISA: Enzyme-linked Immunosorbent Assay, IF: Immunofluorescence, WB: Western blot, IP: Immunoprecipitation.

2.6 | RNA extraction and real time PCR

Total RNA was extracted using TRIzol reagent (Cat 15596026; Invitrogen – Thermo Fisher Scientific, Waltham, MA) following manufacturer's instruction. Briefly, 1 mL of TRIzol was used to homogenize the tissues and, after 5 min of incubation at RT, 0.2 mL of chloroform was added. Following centrifugation (12,000*g* for 15 min at +4°C), the aqueous phase was collected into fresh tubes and the RNA was precipitated with 0.5 mL of isopropyl alcohol. Samples were centrifuged, the pellet washed with 75% ethanol and after a further centrifugation, RNA pellet was dried and then redissolved with RNAse free water for 10 min a 55°C. RNA samples' concentrations and purity were evaluated by spectrophotometer at λ = 260/280 nm and λ = 260/230 nm. Only samples with λ260/λ280 ratio >1.8 were included in the study. The purified RNA samples were used for the cDNA synthesis (1 μg mRNA/sample; QuantiTect Reverse Transcription, cat 205311, Quiagen, Hilden, Germany) and used to measure the expression levels of proNGF-A and proNGF-B. To check for the presence of proNGF-A and proNGF-B transcripts in the rat tissues, we designed specific PCR primers, based on the sequences published at http://www.ensembl.org/Rattus_norvegicus/Transcript/Summary?db=core;g=ENSRNOG00000016571;r=2:204886202-204939523;t=ENSRNOT00000078376. We thus detected the mRNA region spanning from 157 to 285 of the mRNA transcript Ngf-202 (rat proNGF-A; forward: 5′-GTGTCCACCCATCTGCTAGG-3′; reverse: 5′-CACTGAGGTGAGCTTGGGTC-3′; product length 129 bp; custom Applied Biosystem assay AP322XX, Invitrogen corporation, Carlsbad, CA) and region spanning from 9 to 113 of the mRNA transcript Ngf-201 (rat proNGF-B; forward: 5′-CCTGGAGCCGAAGGGGAG-3′; reverse: 5′-CACTGAGGTGAGCTTGGGTC-3′; product length 105 bp; custom Applied Biosystem assay AP47WHV). Real-time PCR was performed on the PCR system CFX96™ Connect (Bio-rad, Hercules, CA), using TaqMan assay (Applied Biosystems). Commercially available Applied Biosystems assays-on-demand reagents were used to measure the expression of rat TrkA (Cat. Nr. Rn573120), p75^{NTR} (Cat. Nr. Rn561634), and β-actin (housekeeping control; Cat Nr. Rn4352660) mRNAs. A standard curve of fourfold serial dilution was prepared with cDNA sample and reaction efficiency was calculated using the equation $=10^{(-1/\text{slope})}$ from the slope of the standard curve (Pfaffl, 2001). Relative quantification was performed using the comparative Ct method and results were expressed as fold induction of controls. Relative expression ratio of the genes of interest were calculated based on the experimentally determined amplification efficiencies, and then normalized for the house-keeping gene following the formula proposed by M.W. Pfaffl (Pfaffl, 2001) that is:

$$E_{\text{gene}}{}^{\Delta\text{Ct (mean of controls-sample)}} / E_{\text{house-keeping}}{}^{\Delta\text{Ct (mean of controls-sample)}}$$

In all experiments, each sample was analyzed in triplicate, and no-template controls and no-reverse transcription controls were run.

2.7 | Protein extraction and western blot

Tissues were homogenized in 50 volumes of ice-cold lysis buffer (Hepes 20 mM pH 7.9; 150 mM sodium chloride; 1% (vol/vol) Nonidet-40; 0.1 mM EDTA; 0.1 mM EGTA; protease and phosphatase inhibitors and centrifugated at ~14,000*g* for 10 min at +4°C. Proteins were treated with 4X reducing sample loading buffer (62.5 mM Tris HCl pH 6.8, 20% (vol/vol) glycerol, 2% (wt/vol) SDS, 0.025% (wt/vol) bromophenol blue, and 100 mM dithiothreitol), boiled at 95°C for 5 min and resolved in 12% SDS-PAGE at 25–30 mA in running buffer (25 mM Tris HCl pH 8.3, 190 mM Glycine, 0.1% SDS). Proteins were blotted onto nitrocellulose membrane (cat 9004-70-G, Bio-rad, Hercules, CA) ON at 30 V in blotting buffer (25 mM Tris HCl pH 8.3, 190 mM Glycine, 20% methanol). Blots were then blocked in PBS + 1% (vol/vol) Tween 20 (PBST) containing 5% (wt/vol) nonfat dry milk 1 hr at RT and then incubated with the

primary antibodies (see Table 1). The blotted membranes were then washed four times with PBST at RT, incubated with respective horseradish peroxidase (HRP)-labeled secondary antibodies (Table 1, Cell Signaling Technology, Danvers, MA). Membranes were incubated with the enhanced chemiluminescence's HRP-substrates (cat. WBKLS0500, Millipore, Burlington, MA) and developed with high performance chemiluminescence film (cat 11666657001, Roche Diagnostic, Mannheim, Germany). Gel densitometry was performed on scanned immunoblot images using the ImageJ gel analysis tool (https://imagej.nih.gov/ij/).

2.8 | Immunoprecipitation

Five-hundred micrograms of total protein extracts were precleared for 1 hr with protein A/G Sepharose (cat. 20421, Pierce Biotechnology, Thermo Fisher Scientific, Waltham, MA) and then immunoprecipitated overnight at 4°C with 2 μg fresh protein A/G Sepharose beads bound to the antibody of interest (Table 1) and then blocked with PBS + 1% BSA for 30 min at RT. Protein A/G-bound immunocomplexes were then washed three times with lysis buffer, suspended in loading buffer and boiled at 95–100°C for 5 min to denature the protein and separate it from the Ab-protein A/G Sepharose bead complex. Samples were then loaded in SDS-PAGE and processed for western blot.

2.9 | ProNGF and mNGF ELISA

To measure the proNGF and mature NGF (mNGF) content in tissue homogenates, we used recently developed specific ELISAs (Soligo et al., 2015). Briefly, the capture antibody was incubated ON at RT, into the wells of Nunc™ MaxiSorp™ ELISA Plates (cat 439454, Thermo Fisher Scientific, Waltham, MA). After blocking 1 hr at RT with PBS + 1% (wt/vol) BSA, the plate was rinsed with PBST and samples incubated for 2 hr at RT. The microwells were then rinsed three times and incubated with detection antibodies dissolved in blocking buffer for 2 hr at RT. Following three washes to remove unbound detection antibody, HRP-conjugated antibody diluted in blocking buffer was added and incubated for 1 hr at RT. To visualize antibody reactivity the chromogenic substrate 3′,3′,5′,5′-tetramethylbenzidine (TMB, cat. T8768, Sigma-Aldrich, St. Louis, MO) was used and color development was stopped by adding 1 N HCl. The colorimetric reaction was measured in absorbance mode at 450 nm by a Multiskan EX ELISA reader (Thermo Fisher Scientific, Waltham, MA).

2.10 | Statistics

Statistical analyses were performed using GraphPad Prism 5 (GraphPad Software, La Jolla, CA). According with the experimental design, data were analyzed by one-way ANOVA and multiple comparisons by Bonferroni post hoc test was chosen as the most conservative procedure to evaluate significant differences between groups (Armstrong, 2014). Data are presented as mean ± *SEM*. p-values < 0.017 were considered statistically significant. Reported p-values were adjusted for multiple comparisons.

3 | RESULTS

3.1 | The balance between mature and proNGF and between different proNGF variants are modulated by electroacupuncture in diabetic rats

Different proNGF mRNAs are expressed in mouse tissues, resulting from alternative splicing and/or activation of different promoters (Edwards, Selby, & Rutter, 1986; Racke, Mason, Johnson, Brankamp, & Linnik, 1996). Two main active protein variants are produced (Figure 1a): the longer proNGF-A (molecular mass: 32–34 kDa) and the shorter proNGF-B (molecular mass: 25–27 kDa) (Hempstead, 2014). To investigate whether the two main transcripts are also expressed in rat brain, we designed specific qPCR assays and performed gene expression analysis by RT-PCR (Figure 1b,d). proNGF-A mRNA decreased in diabetic rats' hippocampi, compared to controls (Figure 1b) and EA improved this decrease, although not restoring basal values (Figure 1b). Differently, the proNGF-B mRNA expression was affected neither by STZ nor by EA treatments (Figure 1c). The proNGF-B/proNGF-A mRNA ratio, although not reaching statistical significance, displayed a tendency to increase (at least twofold) in the diabetic rats, regardless of the treatment with EA (Figure 1d). The mNGF/proNGF ratio could characterize the onset and progression of neurodegeneration in diabetes (Soligo et al., 2015). We, therefore, analyzed proNGF and mNGF protein content in the hippocampus by selective ELISA assays (Soligo et al., 2015). ProNGF showed a tendency to increase in diabetic rats (Figure 1e) while mNGF showed the opposite tendency (Figure 1f). Extending our previous findings, we found that the mNGF/proNGF ratio significantly decreased 4 weeks after diabetes induction and that EA returned it to the basal proportion (Figure 1g). When we analyzed the levels of the different hippocampal proNGF variants we found that proNGF-A was neither altered by diabetes nor by EA (Figure 1h,i). Besides, STZ induced a significant threefold increase in proNGF-B, which was counteracted by EA (Figure 1h,i). Overall these data indicate that alteration in the physiological balance between proNGFs transcripts and protein variants could be one of the factors possibly responsible for the loss of the cholinergic phenotype in diabetic rats' brain (see below).

3.2 | Number of proNGF immunopositive hippocampal astrocytes and neurons is increased by diabetes

We analyzed, by confocal microscopy, the possible cellular source of proNGF in the hippocampus of control, STZ and STZ + EA rats. Automated image analysis performed by the Imaris Bitplane™ software, revealed that astrocytes, immunolabeled for the cell-specific marker GFAP (Figure 2a) and characterized by the typical stellate form, increased in the DG of diabetic rats, compared to controls (Figure 2b). This number remained elevated also after EA (Figure 2b), indicating that the prolonged proinflammatory response induced by STZ was not corrected by the physical therapy. These results complete our previously published observations, which reported a decrease in the number of granular neurons in diabetic rats DG, successively rescued by EA (Soligo et al., 2017). A number of astrocytes ($GFAP^+$) (Figure 2c) and numerous neurons ($NeuN^+$), within the hilus and the granular

layer (Figure 2d), were also proNGF$^+$. However, the analysis of the proNGF content in both neurons and astrocytes, automatically discriminated by the Imaris software and expressed as percentage of proNGF$^+$ mean fluorescence intensity (MFI) in each cell population over the total MFI (Figure 2e,f), did not reveal significant variations in proNGF MFI in the cytoplasm of both cell populations but only a tendency to increase after STZ treatment, that was not affected by EA (Figure 2e,f).

3.3 | GFAP-expressing cell number is increased in the medial septum after diabetes induction

One main physiological role of NGF in the central nervous system (CNS) is to provide neurotrophic support for BFCN cholinergic neurons (Hefti, 1986). Thus, we investigated whether the effects of diabetes and EA on mNGF/proNGF paralleled changes in MS morphology (Figure 3), in the cholinergic phenotype of MS neurons (Figure 4) and in MS content and distribution of NGF receptors (Figure 5). The total cell number in MS, evaluated by nuclear Hoechst labeling, significantly increased in STZ-treated rats compared to controls (Figure 3a,b), while no differences were observed in STZ + EA group (Figure 3a,b). To verify whether to be increased were neurons or glial cells, we counted the number of cells expressing either the neuronal cell marker NeuN (Figure 3c,d) or the glial cell marker GFAP (Figure 3e,f). No significant differences were observed in the number of NeuN$^+$ cells among all experimental groups (Figure 3c,d), while diabetes induced a significant increase in the number of GFAP$^+$ cells, which decreased, although not at the control levels, after EA (Figure 3e,f). These results indicate that STZ treatment mainly increases the number of glial cells in MS, suggesting a neuroinflammatory response, as observed in other models of septo-hippocampal damages (Gage, Olejniczak, & Armstrong, 1988; Shoham, Bejar, Kovalev, Schorer-Apelbaum, & Weinstock, 2007).

3.4 | Electroacupuncture rescues the cholinergic phenotype in medial septum neurons of diabetic rats

The number of neurons expressing ChAT (Figure 4a–d) (Cimino et al., 1996), a specific cholinergic marker, whose expression is directly regulated by NGF (Pongrac & Rylett, 1998), was analyzed by confocal microscopy. Diabetic rats bared a significant decrease in the number of MS ChAT$^+$ neurons compared to healthy controls and EA restored control values (Figure 4b,c). ChAT protein levels in immunopositive cells significantly decreased in STZ-treated rats returning to control levels after EA (Figure 4b,d), as observed for the number of immunopositive cells. We, then, investigated whether the effects of diabetes and EA on MS ChAT-expressing cells were paralleled by alterations in the cholinergic fibers, which originate from MS neurons and, through the *fimbria* (Figure 4a), innervate the hippocampus (Figure 4e–j). After diabetes induction, there was a nonsignificant reduction in the area occupied by cholinergic fibers departing from MS, while EA induced a substantial increase in cholinergic fibers in diabetic animals (STZ vs. STZ + EA: Figure 4f). The ChAT$^+$ fibers MFI, however, was not affected by experimental procedures (Figure 4g). Finally, we measured the area reached by ChAT$^+$ *fimbria* fibers at hippocampal level (Figure 4h–j). Although ANOVA revealed a significant effect of the experimental treatments ($p = 0.0118$, $F_{2,34} = 5.07$) multiple comparison analysis did not show significant differences among experimental groups (Figure 4i). On the other hand, ChAT MFI decreased in STZ group and did not improve after EA (Figure 4j). Overall, these results confirmed a cholinergic dysfunction in diabetic rats BFCN (Rocco et al., 2013; Welsh & Wecker, 1991) and suggested that EA could rescue the cholinergic phenotype, recovering ChAT production in the MS neurons and partially rescuing its transport toward the hippocampus, were acetylcholine is synthesized in nerve terminals, by preserving the amount of cholinergic fibers entering the *fimbria* bundle.

3.5 | Electroacupuncture counteracts the diabetes-induced variation in p75^{NTR} mRNA expression and in the number of p75^{NTR}-expressing cells in the medial septum

MS neurons express both main NGF receptors, TrkA and p75^{NTR}, that, after challenging mNGF/proNGF (Hempstead, 2006) elicit either neurotrophic or apoptotic outcome (Masoudi et al., 2009). TrkA mRNA relative expression, measured by RT-PCR on isolated MS, was unaffected by STZ and EA (Figure 5a), while p75^{NTR} mRNA significantly decreased in diabetic rats after the treatment with EA (Figure 5b). The analysis of p75^{NTR} and TrkA MFI showed no differences in the overall tissue content of both receptors (Figure 5d,g) as shown by the representative images of MS slices immunolabeled for TrkA or p75^{NTR} (Figure 5c,f). While the number of TrkA$^+$ cells was unaffected by experimental diabetes and EA (Figure 5e), p75^{NTR+} cells decreased in STZ group, compared to controls, and recovered in STZ + EA group (Figure 5h). Thus, EA was effective in counteracting the diabetes-induced reduction in the total number of cells in the MS that respond to NGF and proNGF by challenging p75^{NTR}.

3.6 | TrkA content in cholinergic neurons of the medial septum is decreased by diabetes and normalized by electroacupuncture

The following step was to study NGF receptors specifically expressed in the cholinergic neurons of the MS. Representative images of TrkA/ChAT and p75^{NTR}/ChAT double labeled cells are shown in Figure 6a,b. The content of TrkA receptors, measured as MFI, significantly decreased in cholinergic neurons of diabetic rats, an effect counteracted by EA (Figure 6c). The same analysis performed for the p75^{NTR} receptor showed no differences among the experimental groups (Figure 6d). These data suggest that, in the diabetic brain, differently from what observed for other cell types in the MS (Figure 5), cholinergic neurons modulate their responsivity to mNGF/proNGF by decreasing the amount of TrkA receptor, while not changing their ability to respond to proNGF through the p75^{NTR} receptor (Nykjaer, Willnow, & Petersen, 2005). Of note, EA was effective in modifying the potential TrkA-mediated cholinergic neurons responsivity.

4 | DISCUSSION

We aimed at studying the effects of EA on diabetes-induced septo-hippocampal neuronal suffering in a rat model of Type 1 diabetes. We investigated how EA affected cholinergic neurotransmission and

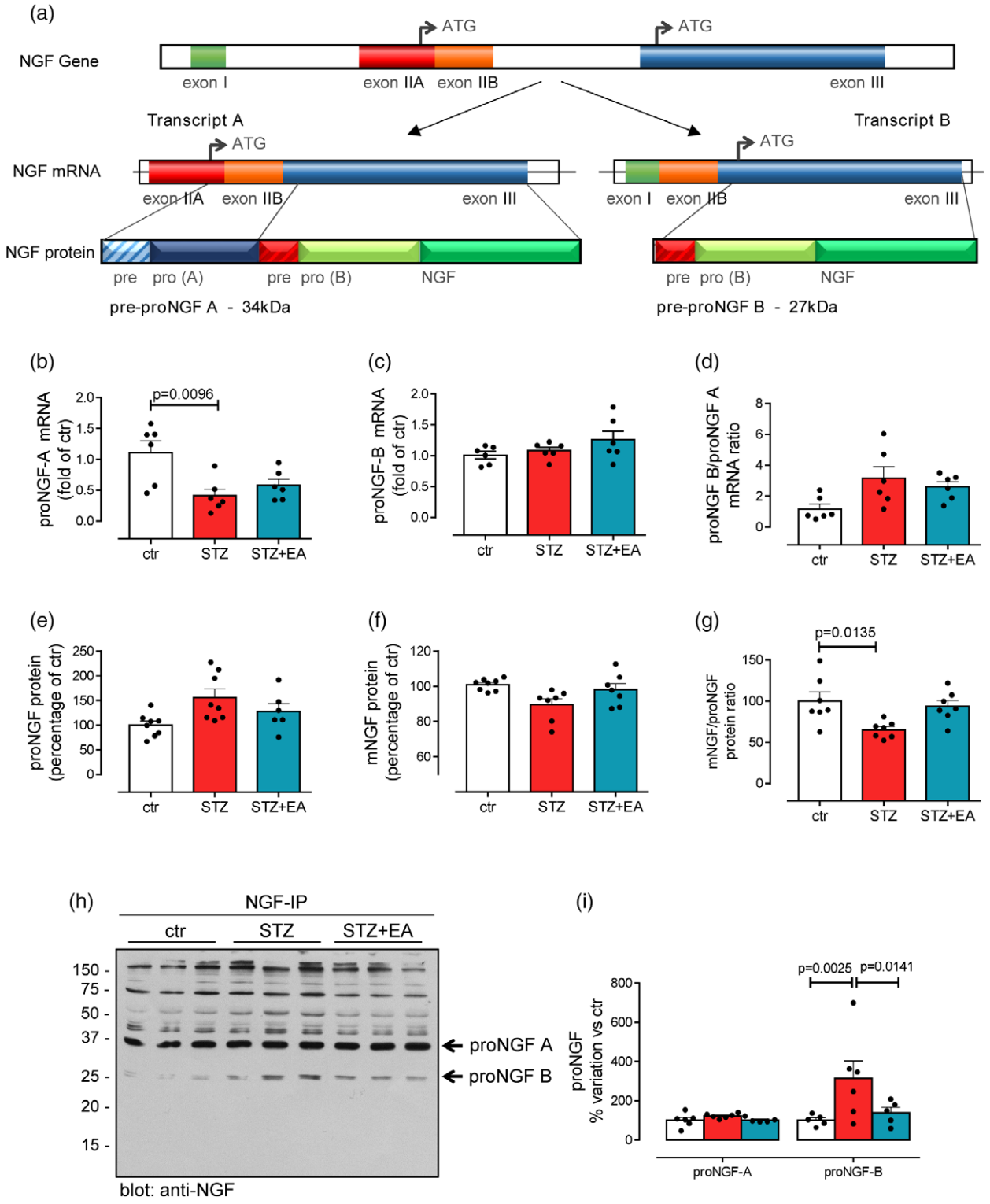

FIGURE 1 Electroacupuncture modulated the diabetes induced increase in the hippocampal proNGF-B/proNGF-A and proNGF/mNGF ratios. (a) Schematic drawing of the *ngf* gene structure in rats (upper line), NGF mRNA splicing variants (transcript A and transcript B; middle lane) that are translated in the two proNGFs protein variants (pre-proNGF-A and pre-proNGF B; lower lane). (b) Relative mRNA expression of proNGF-A, (c) proNGF-B, and (d) the ratio between the two variants in the hippocampus. $n = 6$ rats for each experimental group. (e) proNGF protein, (f) mNGF protein, and (g) the ratio between mNGF and proNGF in the hippocampus. $n =$ min 6, max 8. (h) Representative western blot of anti NGF-immunoprecipitated (NGF-IP) hippocampal extracts. Bands corresponding to proNGF-A and proNGF-B variants are pointed by arrows. (i) Densitometry of two separate blots obtained after NGF-IP. $n = 6$ for each experimental group. Data are mean ± *SEM* of fold or percentage variations of control group. One-way ANOVA followed by Bonferroni's multiple comparisons, *p* values depicted in figure [Color figure can be viewed at wileyonlinelibrary.com]

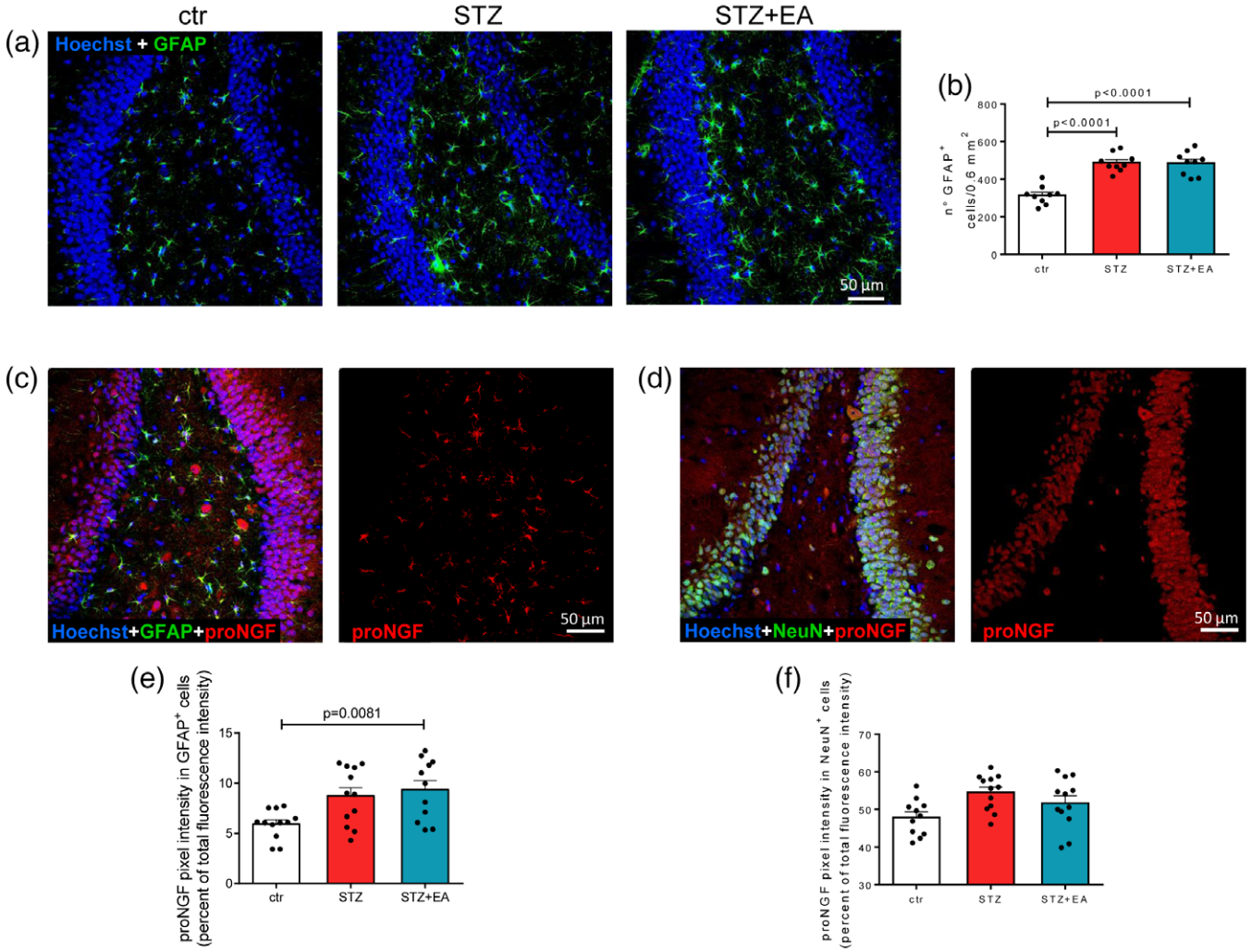

FIGURE 2 ProNGF cellular content is increased in the hippocampus of diabetic rats in both glial and neuronal cells. (a) Immunostaining for GFAP (green) and nuclei (Hoechst; blue) in the dentate gyrus (DG) of controls (ctr), streptozotocin-treated (STZ) and streptozotocin + electroacupuncture-treated (STZ + EA) rats. (b) Quantification of the number of GFAP-expressing cells (astrocytes) in the DG. Values are mean ± *SEM* number of cells in 0.6 mm^2. n = 4 sections × rat, three rats in each experimental group. (c) Immunostaining for GFAP (green), proNGF (red), and nuclei (Hoechst; blue) in the DG. (d) Immunostaining for NeuN (green), proNGF (red), and nuclei (Hoechst; blue) in the DG. (e) Quantification of proNGF content in GFAP-expressing cells in the DG. Data are mean ± *SEM* of the percentage of proNGF pixel intensity over the total cellular fluorescence intensity. n = 4 sections × rat, three rats in each experimental group. (f) Quantification of proNGF content in NeuN-expressing cells in the DG. Data are mean ± *SEM* of the percentage of proNGF pixel intensity over the total cellular fluorescence intensity. n = 4 sections × rat, three rats in each experimental group. Data obtained by one-way ANOVA followed by Bonferroni's multiple comparisons, p values depicted in figure [Color figure can be viewed at wileyonlinelibrary.com]

hippocampal production of proNGF and mNGF, which activity could be dysregulated by diabetes (Rocco et al., 2013; Soligo et al., 2015). The main results were that EA was effective in recovering the diabetes-induced cholinergic cells loss in MS and the cholinergic fibers loss in hippocampus. We found an increased number of astrocytes in diabetic brain, which could embody a suitable source for the increased proNGF production, while EA in diabetic animals restored both normal glial/neurons and mNGF/proNGF ratios. Of notice, the neurodegenerative picture developing after diabetes induction and normalized after EA treatment, was characterized by the selective impairment in the proNGF-B variant.

EA is a physical therapy able to regulate the septo-hippocampal physiology (Ho et al., 2014; Nam, Ahn, & Choi, 2013; Rocco et al., 2013; Soligo et al., 2017). EA modulates both the peripheral and central processing of sensory information (Andersson & Lundeberg, 1995; Lewith, White, & Pariente, 2005). The hippocampus integrates sensory information driven from cortical areas, midbrain, and brainstem, these latter conveyed through basal forebrain cholinergic neurons (Khakpai, Nasehi, Haeri-Rohani, Eidi, & Zarrindast, 2013). Therefore, EA could affect hippocampal functions by modulating both subcortical and cortical hippocampal inputs. It is conceivable that hippocampal neurons could benefit from the activation of sensory processes exerted by EA, improving neural plasticity, which stimulates the recovery of the diabetes-impaired cholinergic transmission, and normalizing proNGF/mNGF release and activity.

EA was effective in regulating the proNGF/mNGF ratio, unbalanced in diabetic brain (Soligo et al., 2015). We found that EA restored normal mNGF/proNGF protein ratio by decreasing the tissue content of the proNGF-B protein. Indeed, this represents the main novelty of the present work, as it could represent the initial characterization of a

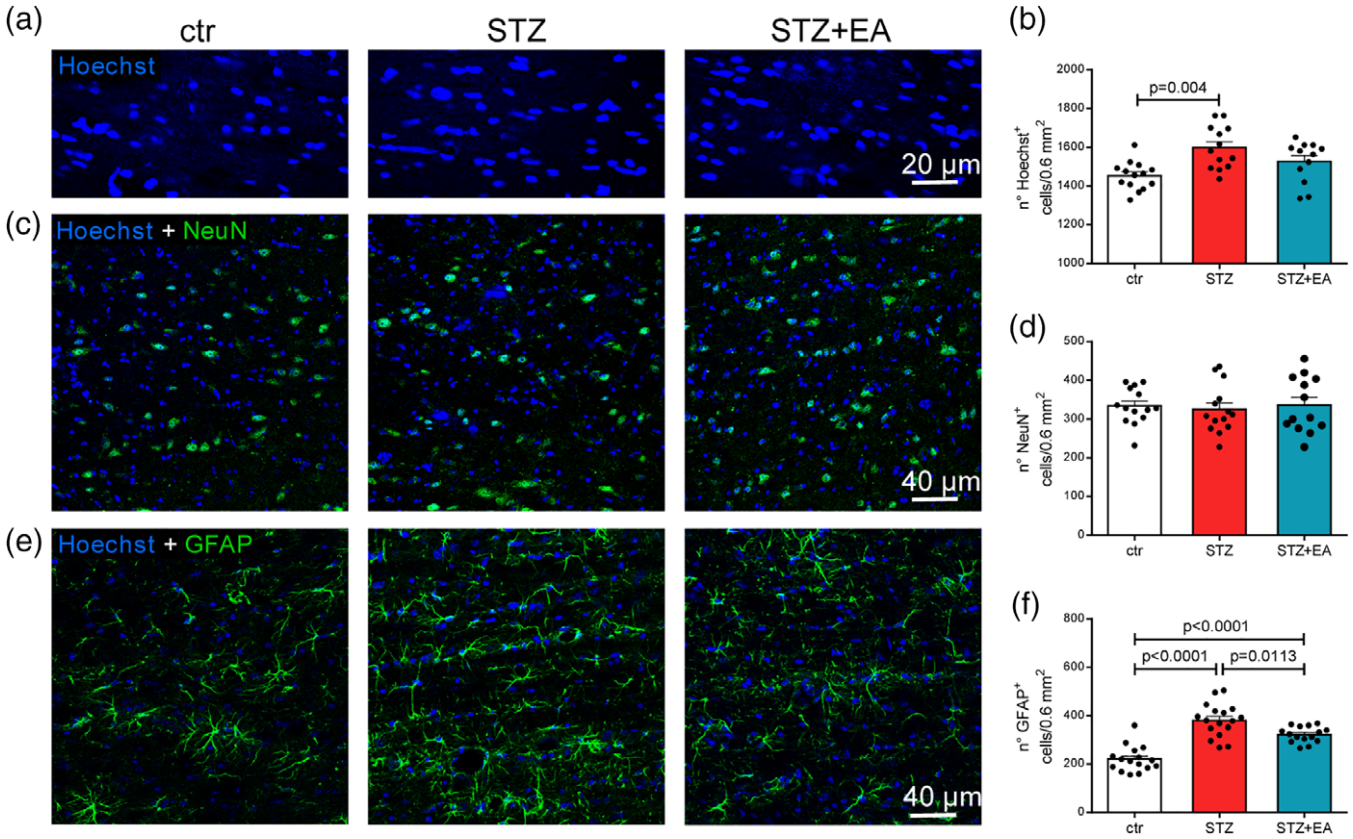

FIGURE 3 GFAP-expressing cells are increased in the medial septum after diabetes induction. (a) Immunostaining for cell nuclei (Hoechst; blue) in the medial septum (MS) of controls (ctr) streptozotocin-treated (STZ) and streptozotocin + electroacupuncture-treated (STZ + EA) rats. (b) Quantification of the number of cells in the MS. Values are mean ± *SEM* number of cells in 0.6 mm^2. *N* = 4–5 sections × rat, three rats in each experimental group. (c) Immunostaining for NeuN (green) and nuclei (Hoechst; blue) in the MS. (d) Quantification of the number of NeuN-expressing cells (neurons) in the MS. Values are mean ± *SEM* number of cells in 0.6 mm^2. *n* = 4–5 sections × rat, three rats in each experimental group. (e) Immunostaining for GFAP (green) and nuclei (Hoechst; blue) in the MS. (f) Quantification of the number of GFAP-expressing cells (astrocytes) in the MS. Values are mean ± *SEM* number of cells in 0.6 mm^2. *n* = 5–6 sections × rat, three rats in each experimental group. Data obtained by one-way ANOVA followed by Bonferroni's multiple comparisons, *p* values depicted in figure [Color figure can be viewed at wileyonlinelibrary.com]

possible differential role played by the two main proNGF variants in the brain. Using specific PCR primers, we detected both proNGF-A and proNGF-B, demonstrating that both mRNA variants are expressed in rat brain. ProNGF-A mRNA was decreased, while proNGF-B expression was not affected by diabetes. However, the increase in the tissue content of proNGF-B protein variant, supports its putative role in the development of neurodegeneration. Previous findings about the ability of such proNGF to challenge the $p75^{NTR}$-sortilin complex and to elicit a proapoptotic response (Hempstead, 2006; Lee, Kermani, Teng, & Hempstead, 2001; Nykjaer et al., 2004) further suggest that a proNGF-B-mediated mechanism could represent an important pathogenic cofactor in the development of diabetes-induced neuronal sufferance. The sensory stimulation by EA could improve the septo-hippocampal physiology making proNGF-B less available for the challenge to $p75^{NTR}$/sortilin complex. At the same time, making mNGF more available (Soligo et al., 2015), EA can influence the observed up-regulation of both ChAT (Hefti, Dravid, & Hartikka, 1984) and TrkA (Zhou, Valletta, Grimes, & Mobley, 1995) in cholinergic neurons, and the improvement in cholinergic metabolism recently reported in the same experimental model (Soligo et al., 2017). Overall, these EA-induced effects could restore the positive feedback loop between NGF and acetylcholine. It is conceivable, indeed, that a link could exist, in the brain of diabetic rats, between the observed EA-induced improvement of cholinergic tone, the described recovery in the functionality of muscarinic receptors in the hippocampus (Soligo et al., 2017) and the rescue of a proper regulation of NGF gene expression and protein processing, both known to be regulated by cholinergic neurotransmission (Bruno & Cuello, 2006; Korsching, Auburger, Heumann, Scott, & Thoenen, 1985).

The possible sources for the increased proNGF in the DG of diabetic rats could be both granular neurons and astrocytes. Granular DG neurons were previously indicated as the main NGF producers in the hippocampus, in physiological conditions (Ayer-LeLievre, Olson, Ebendal, Seiger, & Persson, 1988). We also previously described an increase in proNGF immunoreactivity in the DG granular layer of diabetic rats, associated with a facilitated activity-dependent release of proNGF from diabetic hippocampal slices (Soligo et al., 2017). Nevertheless, GFAP-expressing cells were also pointed as a possible source of NGF in the hippocampus following *fimbria* fornix transection (Gage et al., 1988). Thus, it is conceivable that a consistent amount of proNGF in the hippocampus could be produced as a consequence of the establishment of astrogliosis associated with diabetes (Revsin

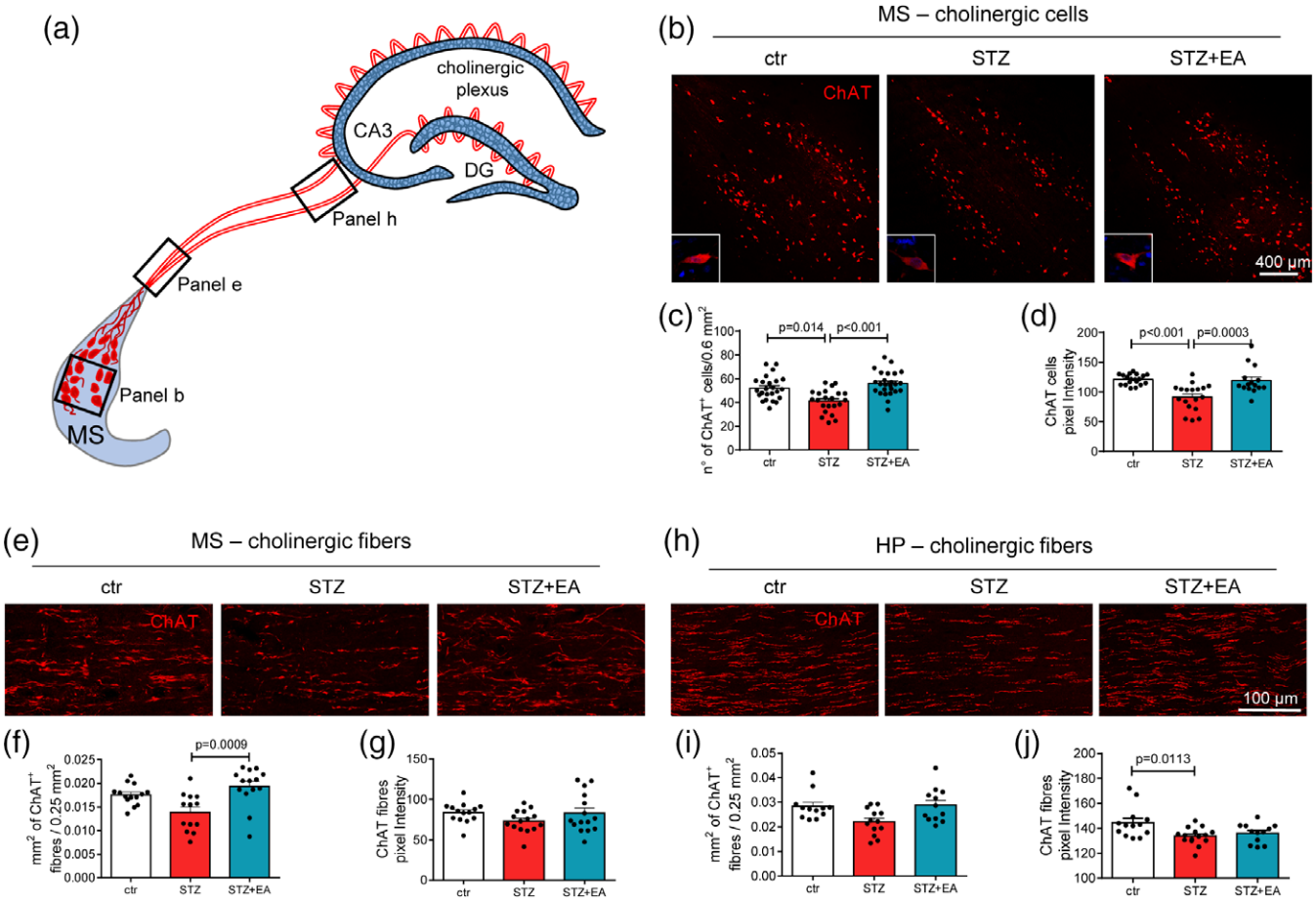

FIGURE 4 Electroacupuncture rescues the cholinergic phenotype in the medial septum neurons of diabetic rats. (a) Schematic drawing showing the septo-hippocampal cholinergic connections through the fimbria. The cholinergic neurons (red) in the medial septum (MS), send their axons to the hippocampal CA3 and dentate gyrus (DG), where cholinergic fibers form a plexus surrounding the pyramidal (CA3) and granular (DG) glutamatergic neurons. Black boxes indicate the areas where quantitative evaluation of choline-acetyl transferase (ChAT)-immunopositive neurons and fibers have been quantified. (b) Immunostaining for ChAT (red) in neurons of the MS. (c) Quantification of the number of ChAT-expressing neurons in the MS. Values are mean ± *SEM* number of cells in 0.6 mm^2. *n* = 4–5 sections × rat, five rats in each experimental group. (d) Quantification of ChAT content in cholinergic neurons of the MS. Data are mean ± *SEM* of the red pixel intensity. *n* = 3–4 sections × rat, five rats in each experimental group. (e) Immunostaining for ChAT (red) in cholinergic fibers arising from the MS. (f) Quantification of the area covered by red immunostaining over 0.25 mm^2. Values are expressed as mean area ± *SEM*. *n* = 3–4 sections × rat, four rats in each experimental group. (g) Quantification of ChAT content in cholinergic fibers arising from MS. Data are mean ± *SEM* of the red pixel intensity. *n* = 3–4 sections × rat, four rats in each experimental group. (h) Immunostaining for ChAT (red) in cholinergic fibers entering the hippocampus. Scale bar, 100 µm. (i) Quantification of the area covered by red immunostaining over 0.25 mm^2. Values are expressed as mean area ± *SEM*. *n* = 3–4 sections × rat, four rats in each experimental group. (j) Quantification of ChAT content in cholinergic fibers. Data are mean ± *SEM* of the red pixel intensity. *n* = 3–4 sections × rat, four rats in each experimental group. Data were obtained by one-way ANOVA followed by Bonferroni's multiple comparisons, *p* values depicted in figure [Color figure can be viewed at wileyonlinelibrary.com]

et al., 2005). We found that EA was ineffective in normalizing the diabetes-induced over-expression of the glial phenotype and in decreasing the NGF immunoreactivity expressed by astrocytes and neurons. Although not specifically addressed by our present work, it is conceivable that EA, by affecting the excitatory and modulatory neurotransmissions conveyed through the hippocampus from entorhinal cortex and the basal forebrain respectively, normalized the proNGF-B protein content and the mNGF/proNGF balance by acting at gene expression and/or at post-translational level (Bruno & Cuello, 2006; Korsching et al., 1985; Soligo et al., 2017). On the other hand, it is also possible to hypothesize that neurons and glia produce different proNGF variants and that the molecular readout that we observed be the result of the yet described EA-promoted DG granular neurons neuroprotection (Soligo et al., 2017), with consequent rescue of the neuronal-produced proNGF variant.

The effects of EA on septo-hippocampal physiology in diabetic animals could reflect the recovery of excitatory (Soligo et al., 2017) and/or modulatory neurotransmission. We found that EA in diabetic rats induced the rescue of cholinergic neurons number and fibers in MS and hippocampus. Damage of the cholinergic system has been associated with neurodegeneration and cognitive decline, such as those observed in DE (Wang et al., 2014; Welsh & Wecker, 1991) and Alzheimer's disease (Mufson, Counts, Perez, & Ginsberg, 2008; Schliebs & Arendt, 2011). We confirmed previous evidence that diabetes in young rats is

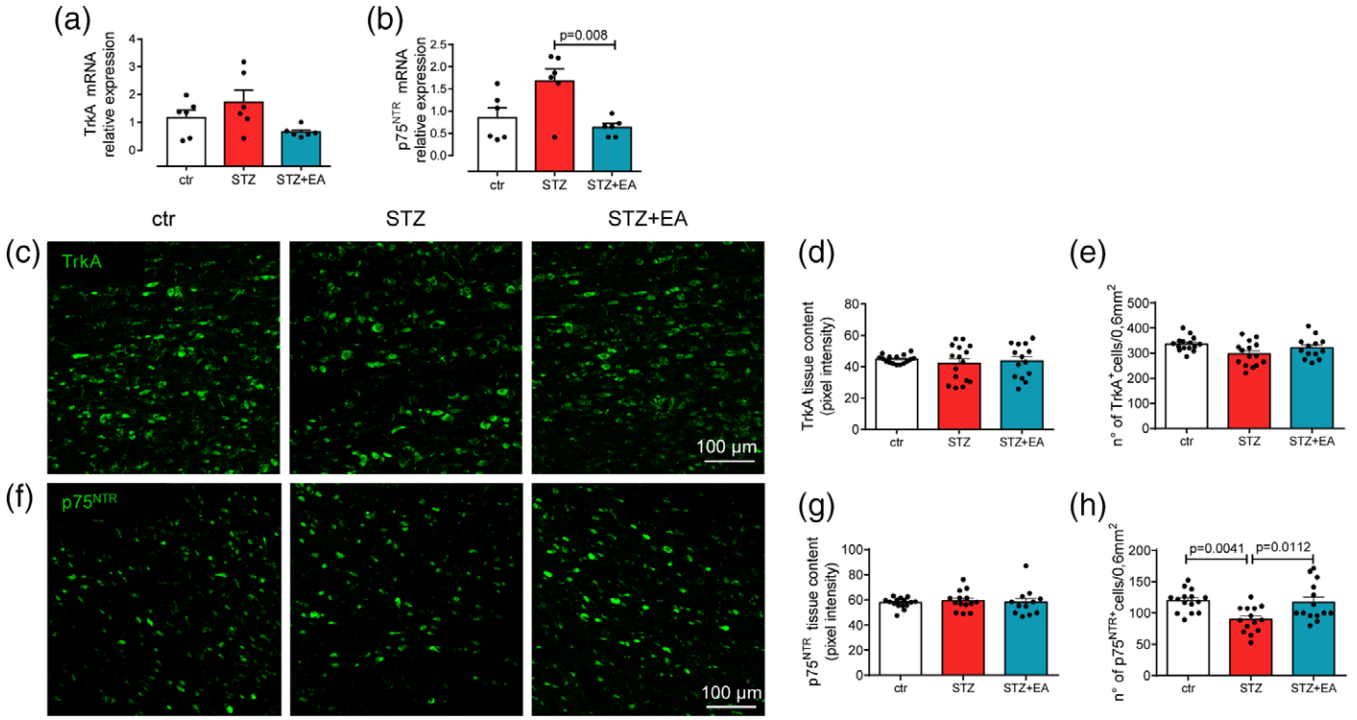

FIGURE 5 Electroacupuncture counteracted the diabetes-induced variation in $p75^{NTR}$ mRNA expression and $p75^{NTR}$-expressing cell number. (a) Relative TrkA-mRNA expression in the medial septum (MS). (b) Relative $p75^{NTR}$-mRNA expression in the MS. $n = 6$ rats in each experimental group. (c) Immunostaining for TrkA (green) in MS neurons of controls (ctr), streptozotocin-treated (STZ), and streptozotocin + electroacupuncture-treated (STZ + EA) rats. (d) Quantification of TrkA tissue content in the MS. Data are mean ± *SEM* of the green pixel intensity. $n = 3$–4 sections × rat, four rats in each experimental group. (e) Quantification of TrkA-expressing cell number in the MS. Data are mean ± *SEM* number of cells in 0.6 mm^2. $n = 3$–4 sections × rat, four rats in each experimental group. (f) Immunostaining for $p75^{NTR}$ (green) in cells of the MS. (g) Quantification of $p75^{NTR}$ tissue content in the MS. Data are mean ± *SEM* of the green pixel intensity. $n = 3$–4 sections × rat, four rats in each experimental group. (e) Quantification of $p75^{NTR}$-expressing cell number in the MS. Data are mean ± *SEM* number of cells in 0.6 mm^2. $N = 3$–4 sections × rat, four rats in each experimental group. Data were obtained by one-way ANOVA followed by Bonferroni's multiple comparisons, *p* values depicted in figure [Color figure can be viewed at wileyonlinelibrary.com]

characterized by a decrease in the number of cholinergic neurons in the BFCN (Rocco et al., 2013). We extended this report by quantifying the amount of nerve fibers conveying the ChAT enzyme from the MS to their terminals in the hippocampus, were biosynthesis of Ach takes place. The observed loss of ChAT-conveying fibers departing from the MS was consistent with a decrease in the ChAT-containing fibers entering the hippocampus and indicative of a functional cholinergic denervation, one of the possible mechanisms underlying the cholinergic impairment observed in neurodegenerative diseases (Cuello et al., 2010). Our results indicate a loss of cholinergic phenotype after diabetes induction, without alteration in the number of total neurons in BFCN. Thus, it is conceivable that EA, as a physical therapy based on the peripheral induction of a consistent activity in the central circuitries conveying sensory information toward the cortical areas, could overcome the functional cholinergic denervation induced by diabetes, rescuing the impaired expression of cholinergic markers in BFCN neurons. We recently obtained data indicating that this could result from the EA-driven recovery of excitatory neurotransmission and of muscarinic modulatory activity in the hippocampus (Soligo et al., 2017), that in turn could normalize mNGF/proNGF metabolism, positively affecting the expression of ChAT and TrkA in the MS (Li et al., 1995; Pongrac & Rylett, 1998).

Notably, previous studies reported a decrease of the basal forebrain neurons, which express $p75^{NTR}$ and TrkA NGF receptors, in experimental DE (Rocco et al., 2013; Soligo et al., 2015), or after cholinergic axotomy in rodents (Lazo, Mauna, Pissani, Inestrosa, & Bronfman, 2010). The observed preferential decrease in TrkA receptor expression in cholinergic neurons after diabetes induction could shift the activity of the proNGF/mNGF system toward that elicited by the challenge of the $p75^{NTR}$. Supporting this hypothesis, previous data indicates that the prosurvival versus the proapoptotic activity of proNGF is strictly dependent upon the relative amount of the two receptors expressed by responsive cells (Ioannou & Fahnestock, 2017; Masoudi et al., 2009). Therefore, our data suggest that in diabetic rat brains, cholinergic cells selectively down-regulate the NGF-receptor type that stimulates ChAT gene expression (Pongrac & Rylett, 1998), while maintaining the responsivity to proNGF through $p75^{NTR}$ unaltered. The observed EA-induced recovery of TrkA expression in cholinergic MS neurons together with the known regulation of TrkA gene expression by NGF (Li et al., 1995) represent another clue about the regulation of NGF metabolism as a main mechanism mediating the effects of EA on brain physiology.

In conclusion, our data indicate that EA may rescue the diabetes-impaired septo-hippocampal physiology and the cholinergic neurotransmission possibly by modulating the proNGF neurotrophin, which

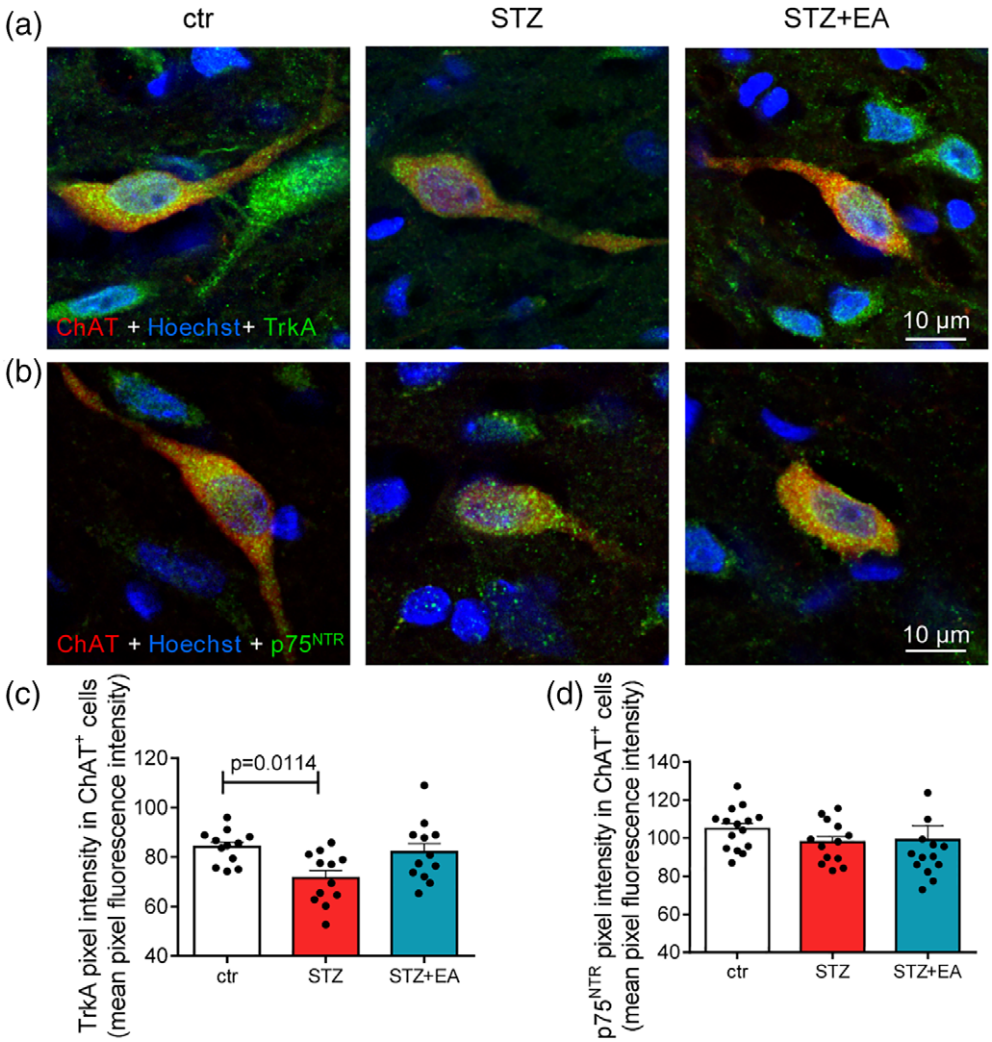

FIGURE 6 TrkA content in cholinergic neurons of the medial septum was decreased by diabetes and normalized by electroacupuncture. (a) Immunostaining for ChAT (red), TrkA (green), and nuclei (Hoechst; blue) in neurons of the medial septum (MS) of controls (ctr), streptozotocin-treated (STZ), and streptozotocin + electroacupuncture-treated (STZ + EA) rats. Scale bar 10 μm. (b) Immunostaining for ChAT (red), $p75^{NTR}$ (green), and nuclei (Hoechst; blue) in neurons of the medial septum (MS) of controls (ctr), streptozotocin-treated (STZ), and streptozotocin + electroacupuncture-treated (STZ + EA) rats. (c) Quantification of the TrkA cellular content in ChAT-expressing cells in the MS. Data are mean ± *SEM* of the percentage of TrkA pixel intensity. n = 3 sections × rat, four rats in each experimental group. (d) Quantification of the $p75^{NTR}$ cellular content in ChAT-expressing cells in the MS. Data are mean ± *SEM* of the percentage of TrkA pixel intensity. n = 3–4 sections × rat, four rats in each experimental group. Data obtained by one-way ANOVA followed by Bonferroni's multiple comparisons, p values depicted in figure [Color figure can be viewed at wileyonlinelibrary.com]

is involved in the maintenance of BFCN phenotype and functions. Our data point at EA as a feasible supportive therapy, with consistent translational value, for cognitive impairments often developing in diabetic patients.

ORCID

Marzia Soligo https://orcid.org/0000-0002-1420-0914
Luigi Manni https://orcid.org/0000-0001-7844-6836

REFERENCES

Aloe, L., & Manni, L. (2009). Low-frequency electro-acupuncture reduces the nociceptive response and the pain mediator enhancement induced by nerve growth factor. *Neuroscience Letters*, *449*(3), 173–177.

Aloe, L., Rocco, M. L., Bianchi, P., & Manni, L. (2012). Nerve growth factor: From the early discoveries to the potential clinical use. *Journal of Translational Medicine*, *10*(1), 239.

Andersson, S., & Lundeberg, T. (1995). Acupuncture - from empiricism to science: Functional background to acupuncture effects in pain and disease. *Medical Hypotheses*, *45*(3), 271–281.

Armstrong, R. A. (2014). When to use the Bonferroni correction. *Ophthalmic & Physiological Optics*, *34*(5), 502–508.

Ayer-LeLievre, C., Olson, L., Ebendal, T., Seiger, A., & Persson, H. (1988). Expression of the beta-nerve growth factor gene in hippocampal neurons. *Science*, *240*(4857), 1339–1341.

Baxter, M. G., Bucci, D. J., Gorman, L. K., Wiley, R. G., & Gallagher, M. (2013). Selective immunotoxic lesions of basal forebrain cholinergic cells: Effects on learning and memory in rats. *Behavioral Neuroscience*, *127*(5), 619–627.

Biessels, G. J., Kappelle, A. C., Bravenboer, B., Erkelens, D. W., & Gispen, W. H. (1994). Cerebral function in diabetes mellitus. *Diabetologia*, *37*(7), 643–650.

Bruno, M. A., & Cuello, A. C. (2006). Activity-dependent release of precursor nerve growth factor, conversion to mature nerve growth factor, and its degradation by a protease cascade. *Proceedings of the National Academy of Sciences of the United States of America*, *103*(17), 6735–6740.

Cimino, M., Cattabeni, F., Di Luca, M., Peruzzi, G., Andena, M., Tirassa, P., … Aloe, L. (1996). Levels of NGF, p75NGFR and ChAT immunoreactivity in brain of adult and aged microencephalic rats. *Neurobiology of Aging*, *17*(1), 137–142.

Cooper-Kuhn, C. M., Winkler, J., & Kuhn, H. G. (2004). Decreased neurogenesis after cholinergic forebrain lesion in the adult rat. *Journal of Neuroscience Research*, *77*(2), 155–165.

Cuello, A. C., Bruno, M. A., Allard, S., Leon, W., & Iulita, M. F. (2010). Cholinergic involvement in Alzheimer's disease. A link with NGF maturation and degradation. *Journal of Molecular Neuroscience*, *40*(1–2), 230–235.

Edwards, R. H., Selby, M. J., & Rutter, W. J. (1986). Differential RNA splicing predicts two distinct nerve growth factor precursors. *Nature*, *319* (6056), 784–787.

Ferreira-Vieira, T. H., Guimaraes, I. M., Silva, F. R., & Ribeiro, F. M. (2016). Alzheimer's disease: Targeting the cholinergic system. *Current Neuropharmacology*, *14*(1), 101–115.

Gage, F. H., Olejniczak, P., & Armstrong, D. M. (1988). Astrocytes are important for sprouting in the septohippocampal circuit. *Experimental Neurology*, *102*(1), 2–13.

Guo, J., Wang, J., Zhang, Z., Yan, J., Chen, M., Pang, T., … Liao, H. (2013). proNGF inhibits neurogenesis and induces glial activation in adult mouse dentate gyrus. *Neurochemical Research*, *38*(8), 1695–1703.

Hefti, F. (1986). Nerve growth factor promotes survival of septal cholinergic neurons after fimbrial transections. *The Journal of Neuroscience*, *6* (8), 2155–2162.

Hefti, F., Dravid, A., & Hartikka, J. (1984). Chronic intraventricular injections of nerve growth factor elevate hippocampal choline acetyltransferase activity in adult rats with partial septo-hippocampal lesions. *Brain Research*, *293*(2), 305–311.

Hempstead, B. L. (2006). Dissecting the diverse actions of pro- and mature neurotrophins. *Current Alzheimer Research*, *3*(1), 19–24.

Hempstead, B. L. (2014). Deciphering proneurotrophin actions. *Handbook of Experimental Pharmacology*, *220*, 17–32.

Ho, T. J., Chan, T. M., Ho, L. I., Lai, C. Y., Lin, C. H., Macdonald, I., … Chen, Y. H. (2014). The possible role of stem cells in acupuncture treatment for neurodegenerative diseases: A literature review of basic studies. *Cell Transplantation*, *23*(4–5), 559–566.

Ioannou, M. S., & Fahnestock, M. (2017). ProNGF, but not NGF, switches from neurotrophic to apoptotic activity in response to reductions in TrkA receptor levels. *International Journal of Molecular Sciences*, *18*(3), E599.

Johansson, J., Yi, F., Shao, R., Lonn, M., Billig, H., & Stener-Victorin, E. (2010). Intense acupuncture normalizes insulin sensitivity, increases muscle GLUT4 content, and improves lipid profile in a rat model of polycystic ovary syndrome. *American Journal of Physiology. Endocrinology and Metabolism*, *299*, E551–E559.

Kaufman, M. P., Longhurst, J. C., Rybicki, K. J., Wallach, J. H., & Mitchell, J. H. (1983). Effects of static muscular contraction on impulse activity of groups III and IV afferents in cats. *Journal of Applied Physiology: Respiratory, Environmental and Exercise Physiology*, *55*(1Pt 1), 105–112.

Khakpai, F., Nasehi, M., Haeri-Rohani, A., Eidi, A., & Zarrindast, M. R. (2013). Septo-hippocampo-septal loop and memory formation. *Basic and Clinical Neuroscience*, *4*(1), 5–23.

Kilkenny, C., Browne, W. J., Cuthill, I. C., Emerson, M., & Altman, D. G. (2010). Improving bioscience research reporting: The ARRIVE guidelines for reporting animal research. *PLoS Biology*, *8*(6), e1000412.

Kniffeki, K. D., Mense, S., & Schmidt, R. F. (1981). Muscle receptors with fine afferent fibers which may evoke circulatory reflexes. *Circulation Research*, *48*(6 Pt 2), I25–I31.

Korsching, S., Auburger, G., Heumann, R., Scott, J., & Thoenen, H. (1985). Levels of nerve growth factor and its mRNA in the central nervous system of the rat correlate with cholinergic innervation. *The EMBO Journal*, *4*(6), 1389–1393.

Lazo, O. M., Mauna, J. C., Pissani, C. A., Inestrosa, N. C., & Bronfman, F. C. (2010). Axotomy-induced neurotrophic withdrawal causes the loss of phenotypic differentiation and downregulation of NGF signalling, but not death of septal cholinergic neurons. *Molecular Neurodegeneration*, *5*, 5.

Lee, R., Kermani, P., Teng, K. K., & Hempstead, B. L. (2001). Regulation of cell survival by secreted proneurotrophins. *Science*, *294*(5548), 1945–1948.

Lewith, G. T., White, P. J., & Pariente, J. (2005). Investigating acupuncture using brain imaging techniques: The current state of play. *Evidence-Based Complementary and Alternative Medicine*, *2*(3), 315–319.

Li, Y., Holtzman, D. M., Kromer, L. F., Kaplan, D. R., Chua-Couzens, J., Clary, D. O., … Mobley, W. C. (1995). Regulation of TrkA and ChAT expression in developing rat basal forebrain: Evidence that both exogenous and endogenous NGF regulate differentiation of cholinergic neurons. *The Journal of Neuroscience*, *15*(4), 2888–2905.

Lund, I., & Lundeberg, T. (2006). Are minimal, superficial or sham acupuncture procedures acceptable as inert placebo controls? *Acupuncture in Medicine*, *24*(1), 13–15.

Lundeberg, T., Lund, I., Sing, A., & Naslund, J. (2011). Is placebo acupuncture what it is intended to be? *Evidence-Based Complementary and Alternative Medicine*, *2011*, 932407.

Manni, L., Aloe, L., & Fiore, M. (2009). Changes in cognition induced by social isolation in the mouse are restored by electro-acupuncture. *Physiology & Behavior*, *98*(5), 537–542.

Manni, L., Florenzano, F., & Aloe, L. (2011). Electroacupuncture counteracts the development of thermal hyperalgesia and the alteration of nerve growth factor and sensory neuromodulators induced by streptozotocin in adult rats. *Diabetologia*, *54*(7), 1900–1908.

Masoudi, R., Ioannou, M. S., Coughlin, M. D., Pagadala, P., Neet, K. E., Clewes, O., … Fahnestock, M. (2009). Biological activity of nerve growth factor precursor is dependent upon relative levels of its receptors. *The Journal of Biological Chemistry*, *284*(27), 18424–18433.

Mohapel, P., Leanza, G., Kokaia, M., & Lindvall, O. (2005). Forebrain acetylcholine regulates adult hippocampal neurogenesis and learning. *Neurobiology of Aging*, *26*(6), 939–946.

Mufson, E. J., Counts, S. E., Perez, S. E., & Ginsberg, S. D. (2008). Cholinergic system during the progression of Alzheimer's disease: Therapeutic implications. *Expert Review of Neurotherapeutics*, *8*(11), 1703–1718.

Nam, M. H., Ahn, K. S., & Choi, S. H. (2013). Acupuncture stimulation induces neurogenesis in adult brain. *International Review of Neurobiology*, *111*, 67–90.

Noguchi, E., Ohsawa, H., Kobayashi, S., Shimura, M., Uchida, S., & Sato, Y. (1999). The effect of electro-acupuncture stimulation on the muscle blood flow of the hindlimb in anesthetized rats. *Journal of the Autonomic Nervous System*, *75*(2–3), 78–86.

Nykjaer A, Lee R, Teng KK, Jansen P, Madsen P, Nielsen MS, Jacobsen C, Kliemannel M, Schwarz E, Willnow TE and others. 2004. Sortilin is essential for proNGF-induced neuronal cell death. *Nature 427*(6977): 843–8.

Nykjaer, A., Willnow, T. E., & Petersen, C. M. (2005). p75NTR--live or let die. *Current Opinion in Neurobiology*, *15*(1), 49–57.

Pagani, L., Manni, L., & Aloe, L. (2006). Effects of electroacupuncture on retinal nerve growth factor and brain-derived neurotrophic factor expression in a rat model of retinitis pigmentosa. *Brain Research*, *1092* (1), 198–206.

Paxinos, G. (1982). *The rat brain in stereotaxic coordinates*. Sydney, Australia: Academic Press.

Pfaffl, M. W. (2001). A new mathematical model for relative quantification in real-time RT-PCR. *Nucleic Acids Research*, *29*(9), e45–e445.

Pongrac, J. L., & Rylett, R. J. (1998). Molecular mechanisms regulating NGF-mediated enhancement of cholinergic neuronal phenotype: c-fos trans-activation of the choline acetyltransferase gene. *Journal of Molecular Neuroscience*, *11*(1), 79–93.

Racke, M. M., Mason, P. J., Johnson, M. P., Brankamp, R. G., & Linnik, M. D. (1996). Demonstration of a second pharmacologically active promoter region in the NGF gene that induces transcription at exon 3. *Brain Research. Molecular Brain Research*, *41*(1–2), 192–199.

Revsin, Y., Saravia, F., Roig, P., Lima, A., de Kloet, E. R., Homo-Delarche, F., & De Nicola, A. F. (2005). Neuronal and astroglial alterations in the hippocampus of a mouse model for type 1 diabetes. *Brain Research*, *1038*(1), 22–31.

Rocco, M. L., Pristera, A., Pistillo, L., Aloe, L., Canu, N., & Manni, L. (2013). Brain cholinergic markers and tau phosphorylation are altered in experimental type 1 diabetes: Normalization by electroacupuncture. *Journal of Alzheimer's Disease*, *33*(3), 767–773.

Sarter, M. (2015). Behavioral-cognitive targets for cholinergic enhancement. *Current Opinion in Behavioral Sciences*, *4*, 22–26.

Sato, A., Sato, Y., & Uchida, S. (2002). Reflex modulation of visceral functions by acupuncture-like stimulation in anesthetized rats. *International Congress Series*, *1238*, 111–123.

Schliebs, R., & Arendt, T. (2011). The cholinergic system in aging and neuronal degeneration. *Behavioural Brain Research*, *221*(2), 555–563.

Shoham, S., Bejar, C., Kovalev, E., Schorer-Apelbaum, D., & Weinstock, M. (2007). Ladostigil prevents gliosis, oxidative-nitrative stress and memory deficits induced by intracerebroventricular injection of streptozotocin in rats. *Neuropharmacology*, *52*(3), 836–843.

Soligo, M., Piccinin, S., Protto, V., Gelfo, F., De Stefano, M. E., Florenzano, F., … Manni, L. (2017). Recovery of hippocampal functions and modulation of muscarinic response by electroacupuncture in young diabetic rats. *Scientific Reports*, *7*(1), 9077.

Soligo, M., Protto, V., Florenzano, F., Bracci-Laudiero, L., De Benedetti, F., Chiaretti, A., & Manni, L. (2015). The mature/pro nerve growth factor ratio is decreased in the brain of diabetic rats: Analysis by ELISA methods. *Brain Research*, *1624*, 455–468.

Stener-Victorin, E., Lundeberg, T., Waldenstrom, U., Manni, L., Aloe, L., Gunnarsson, S., & Janson, P. O. (2000). Effects of electro-acupuncture on nerve growth factor and ovarian morphology in rats with experimentally induced polycystic ovaries. *Biology of Reproduction*, *63*(5), 1497–1503.

Teles-Grilo Ruivo, L. M., & Mellor, J. R. (2013). Cholinergic modulation of hippocampal network function. *Frontiers in Synaptic Neuroscience*, *5*, 2.

Van der Borght, K., Mulder, J., Keijser, J. N., Eggen, B. J., Luiten, P. G., & Van der Zee, E. A. (2005). Input from the medial septum regulates adult hippocampal neurogenesis. *Brain Research Bulletin*, *67*(1–2), 117–125.

Wang, J. Q., Yin, J., Song, Y. F., Zhang, L., Ren, Y. X., Wang, D. G., … Jing, Y. H. (2014). Brain aging and AD-like pathology in streptozotocin-induced diabetic rats. *Journal Diabetes Research*, *2014*, 796840.

Wehrman, T., He, X., Raab, B., Dukipatti, A., Blau, H., & Garcia, K. C. (2007). Structural and mechanistic insights into nerve growth factor interactions with the TrkA and p75 receptors. *Neuron*, *53*(1), 25–38.

Welsh, B., & Wecker, L. (1991). Effects of streptozotocin-induced diabetes on acetylcholine metabolism in rat brain. *Neurochemical Research*, *16*(4), 453–460.

Whittemore, S. R., Friedman, P. L., Larhammar, D., Persson, H., Gonzalez-Carvajal, M., & Holets, V. R. (1988). Rat beta-nerve growth factor sequence and site of synthesis in the adult hippocampus. *Journal of Neuroscience Research*, *20*(4), 403–410.

Zhou, J., Valletta, J. S., Grimes, M. L., & Mobley, W. C. (1995). Multiple levels for regulation of TrkA in PC12 cells by nerve growth factor. *Journal of Neurochemistry*, *65*(3), 1146–1156.

SUPPORTING INFORMATION

Additional supporting information may be found online in the Supporting Information section at the end of this article.

How to cite this article: Protto V, Soligo M, De Stefano ME, et al. Electroacupuncture in rats normalizes the diabetes-induced alterations in the septo-hippocampal cholinergic system. *Hippocampus*. 2019;1–14. https://doi.org/10.1002/hipo.23088